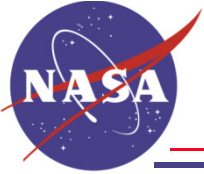


Experimental Evaluation of the “Polished Panel Optical Receiver” Concept on the Deep Space Network’s 34 meter Antenna

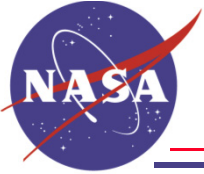
V. Vilnrotter

Jet Propulsion Laboratory
California Institute of Technology



Goal: demonstrate the feasibility of using large aperture “Polished Panel” optical receivers for hybrid RF/Optical deep-space communications via 34-meter DSN antennas

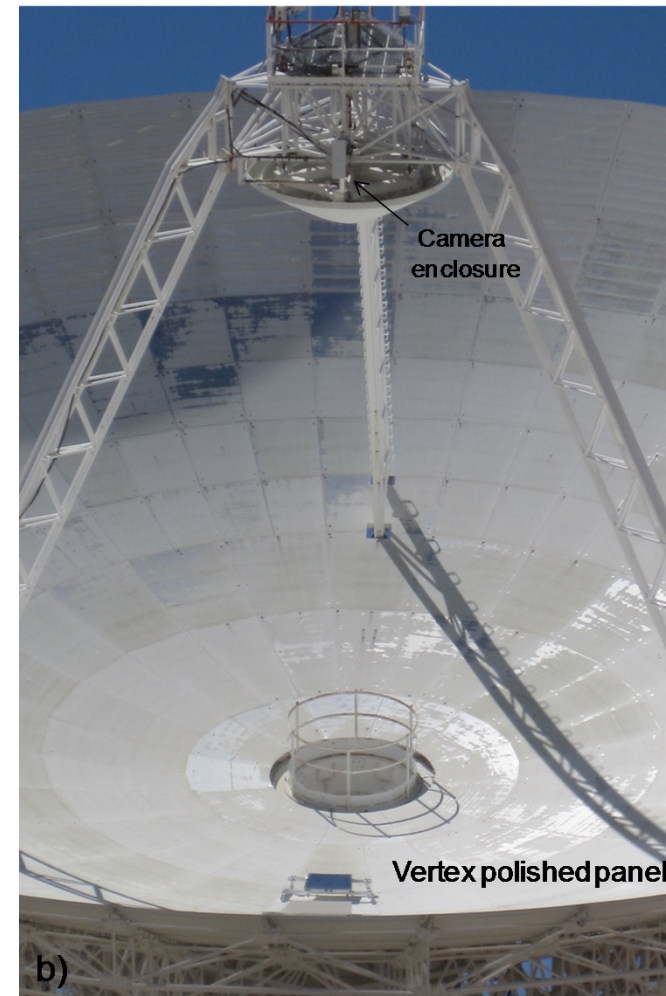
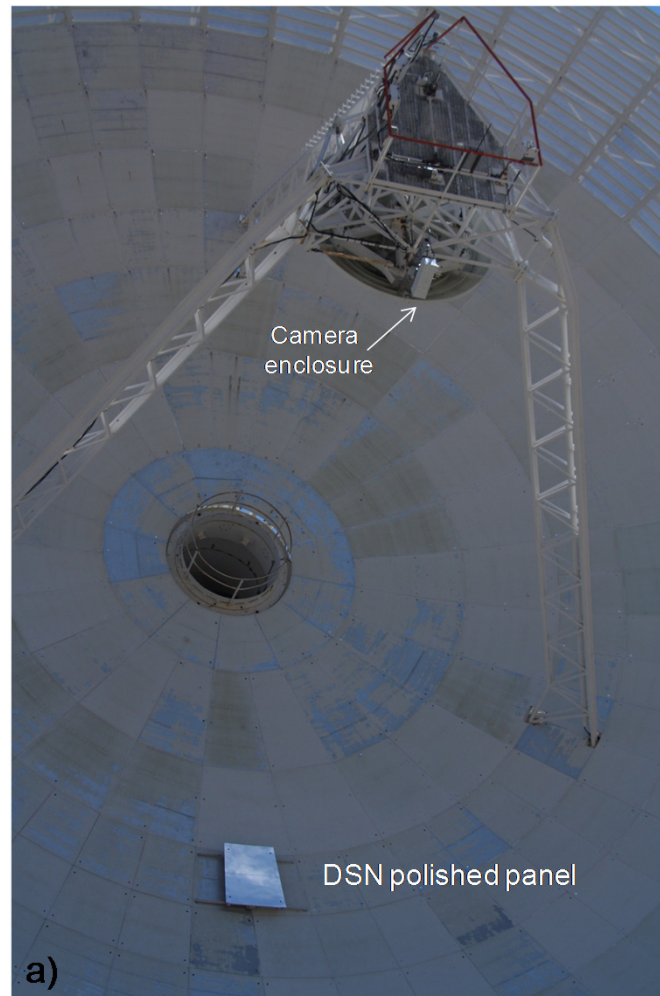
- Installed polished aluminum panels on the main reflector of the 34 meter research antenna at DSS-13, for field evaluation
- Developed and installed a weather-proof remotely controlled camera enclosure on the subreflector support structure
 - Contains a large-sensor camera from Finger Lakes Instruments (FLI)
 - Enclosure and camera are computer controlled from alidade
- Imaged the point-spread-function (PSF) generated by Jupiter
- Developed tracking algorithms based on PSF characteristics
- Evaluated optical communications capabilities based on PSF data



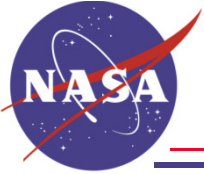
IEEE AEROSPACE CONFERENCE, MARCH 2012

Experimental Evaluation of “Polished Panel Optical Receiver” Concept

Jet Propulsion Laboratory
California Institute of Technology



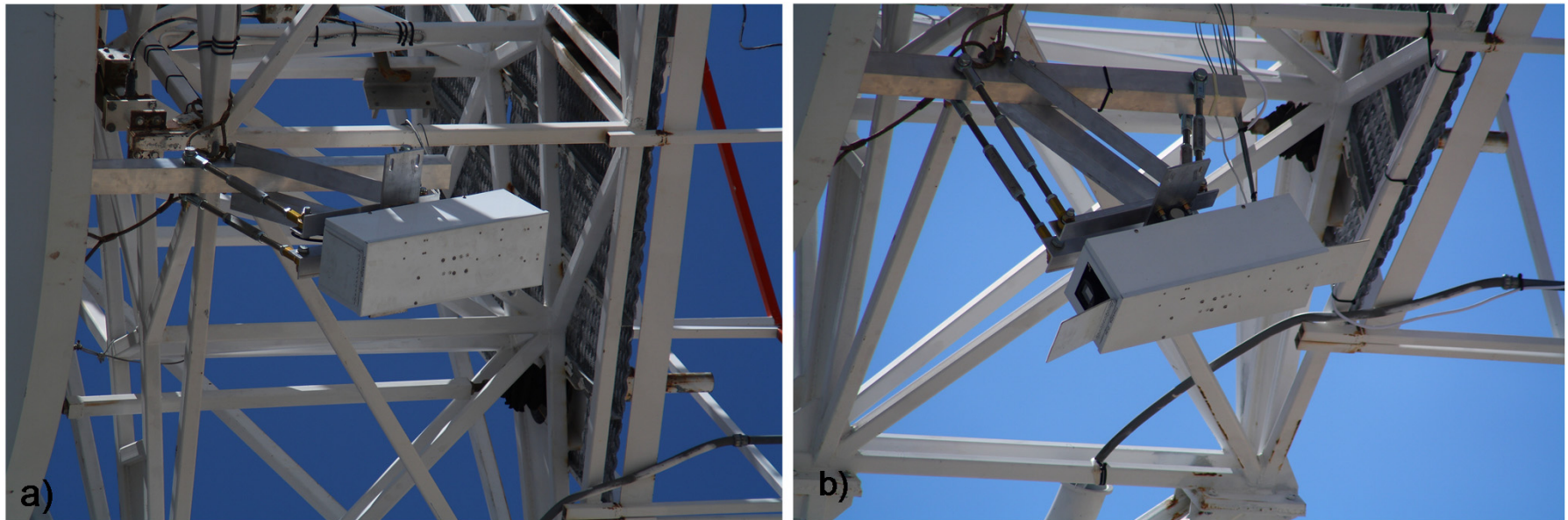
DSN and Vertex Polished Panels mounted on the 34 meter research antenna at DSS-13.
a) DSN polished panel mounted on the main reflector, to help establish weather and dust resistance; b) Vertex polished panel mounted on the main reflector, closer to the center.



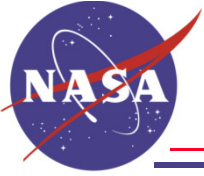
IEEE AEROSPACE CONFERENCE, MARCH 2012

Experimental Evaluation of "Polished Panel Optical Receiver" Concept

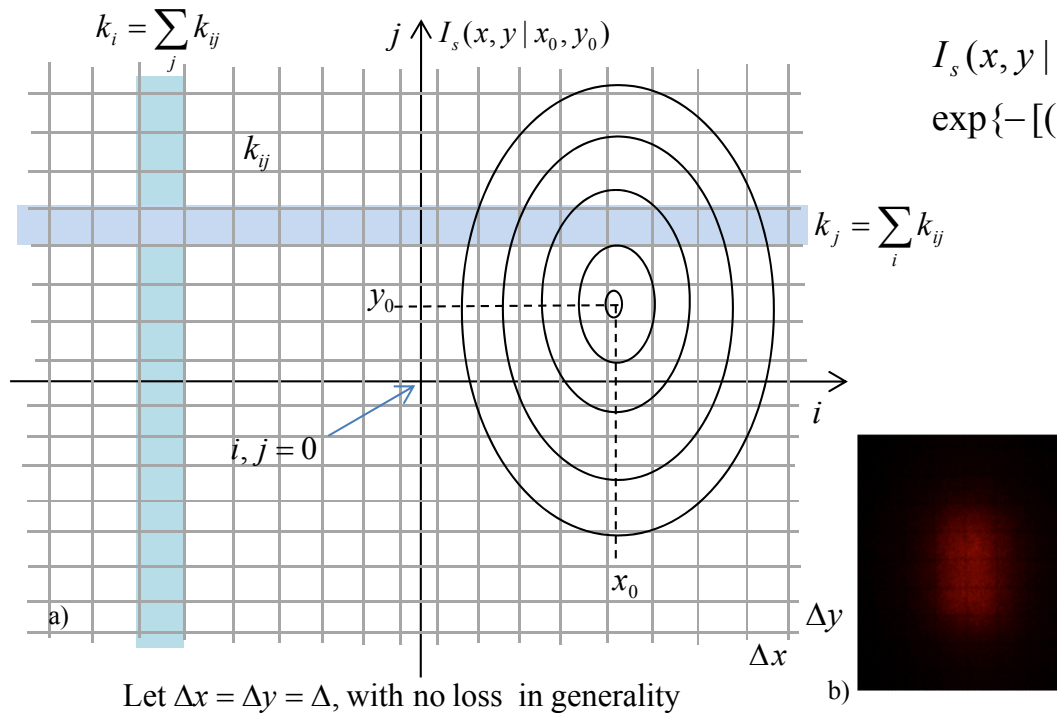
Jet Propulsion Laboratory
California Institute of Technology



**Remote controlled camera enclosure: a) normally closed configuration;
b) open configuration used for data-gathering.**



Mathematical model of Focal-Plane Intensity Distribution



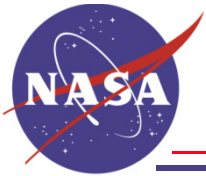
$$I_s(x, y | x_0, y_0) = I_s (2\pi \sigma_s^2)^{-1} \times \exp\{-(x - x_0)^2 / 2\sigma_x^2 + (y - y_0)^2 / 2\sigma_y^2\} \quad \text{watts/cm}^2$$

$$\lambda_s(i, j | x_0, y_0) = \int_0^T P_s(i, j | x_0, y_0) dt \cong T\Delta^2 I_s(i\Delta, j\Delta | x_0, y_0)$$

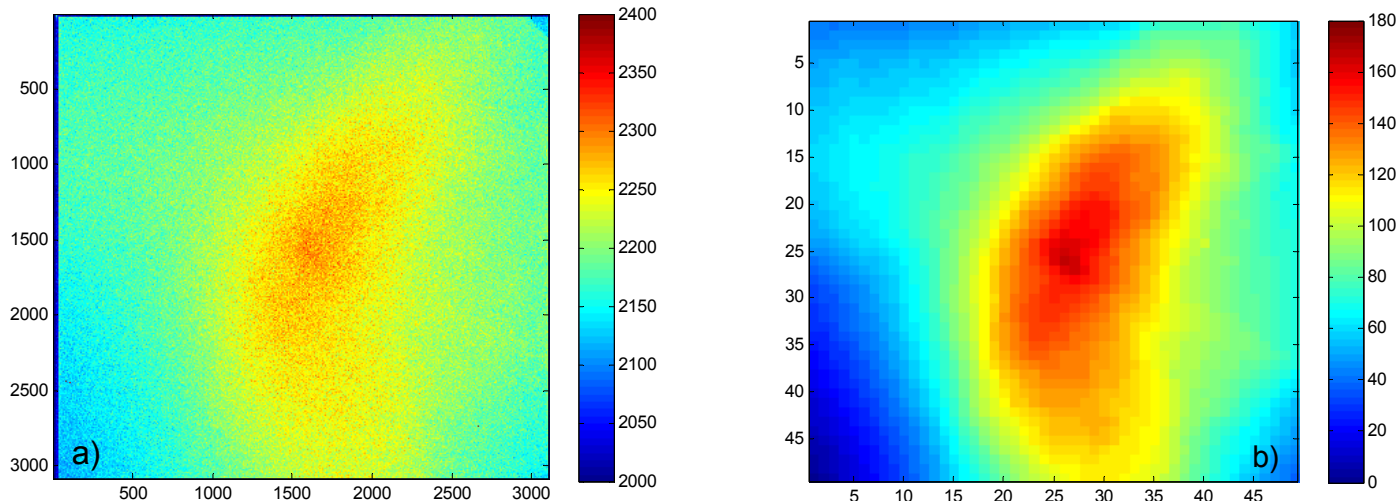
$$p(k_{ij} | x_0, y_0) = [\lambda_s(i, j | x_0, y_0)]^{k_{ij}} \times \exp[-\lambda_s(i, j | x_0, y_0)] / k_{ij}!$$

a) Focal-plane model of pixel array, and elliptical PSF with pointing offsets, motivated by: b) experimentally determined point-spread function (PSF) for the high-quality Vertex panel, photographed on the JPL mesa test range.

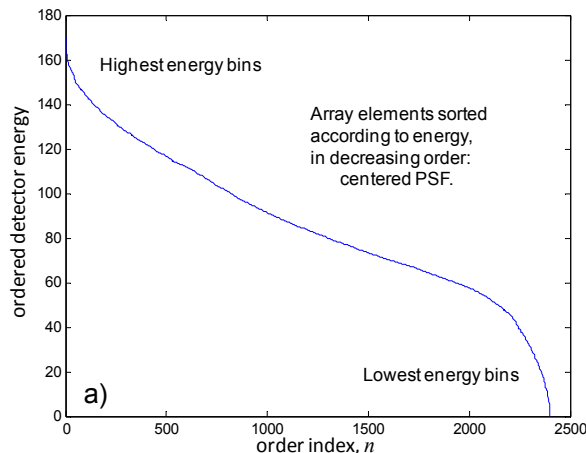
$$p(\mathbf{k} | x_0, y_0) = \prod_{i,j} [\lambda_s(i, j)]^{k_{ij}} \exp[-\lambda_s(i, j)] / k_{ij}!$$



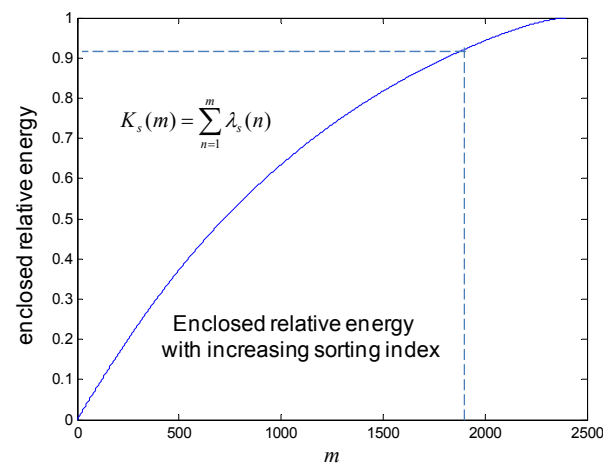
Communications Performance: Experimentally Obtained PSF



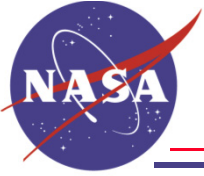
Centered PSF recorded with FLI camera: a) original 10 mega-pixel resolution showing speckle pattern; b) 60X60 binned image emphasizing the spatially averaged structure of the point-spread-function.



Pixels sorted according to energy



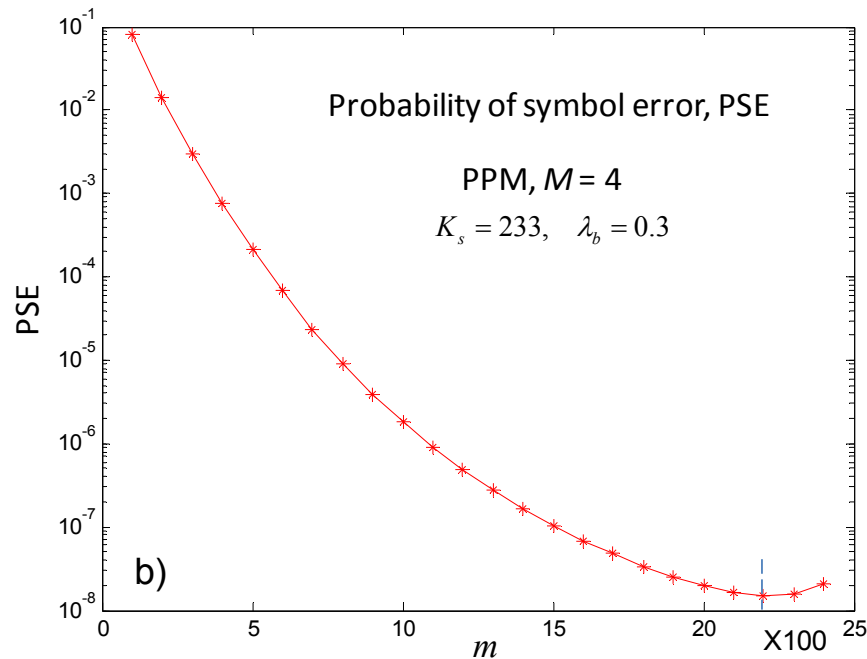
Accumulated energy in first “m” detector elements



Communications Receiver Performance, PPM Signals

$$P_M^l(C) \geq \sum_{k=1}^{\infty} \frac{(K_s(m) + K_b(m))^k}{k!} \exp[-(K_s(R) + K_b(R))] \times \left\{ \sum_{j=0}^{k-1} \frac{(K_b(R))^j}{j!} \exp[-(K_b(R))] \right\}^{M-1}$$

$$P_M^u(E) \equiv 1 - P_M^l(C) \geq P_M(E) \cong P_M(E)$$

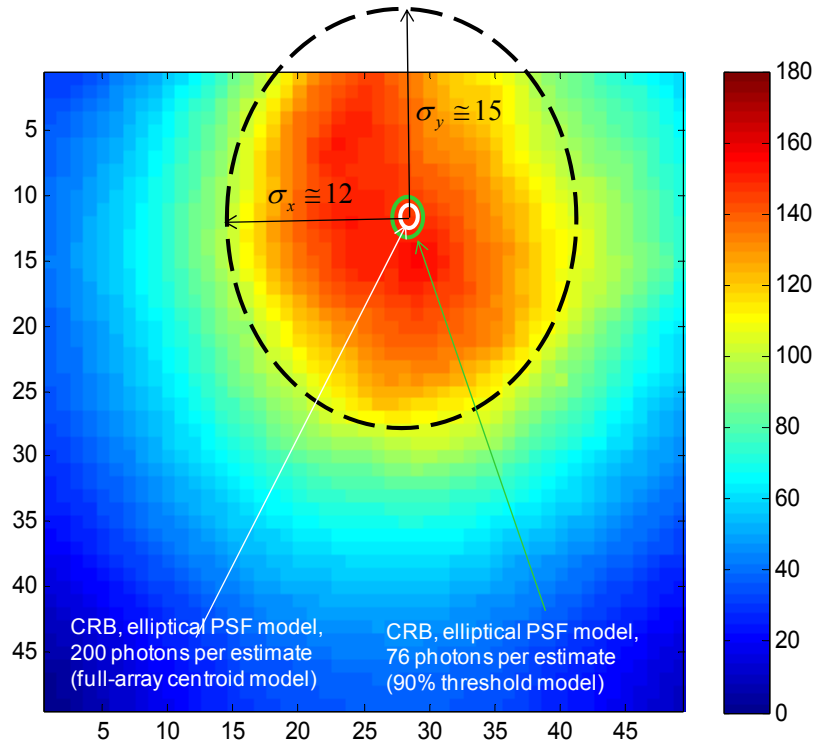
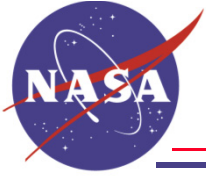


$$K_s(m) = \sum_{n=1}^m \lambda_s(n)$$

$$K_b(m) = m\lambda_b$$

$$P_M(C) \cong \int_{-\infty}^{\infty} dy \operatorname{Gsn}[K_s(m) + K_b(m), y] \times \left[\int_{-\infty}^y dx \operatorname{Gsn}[K_b(m), x] \right]^{M-1}$$

**Probability of symbol error (PSE) with optimal “1, 0” mask,
with background counts of 0.3 photons per slot per bin.**



Estimate of the Cramer-Rao bound for the unmodified and modified threshold algorithms: elliptical PSF with minor axis ~12 bins, major axis ~16 bins.

Centroid Estimator Performance

Several Centroid-estimation algorithms were developed and evaluated:

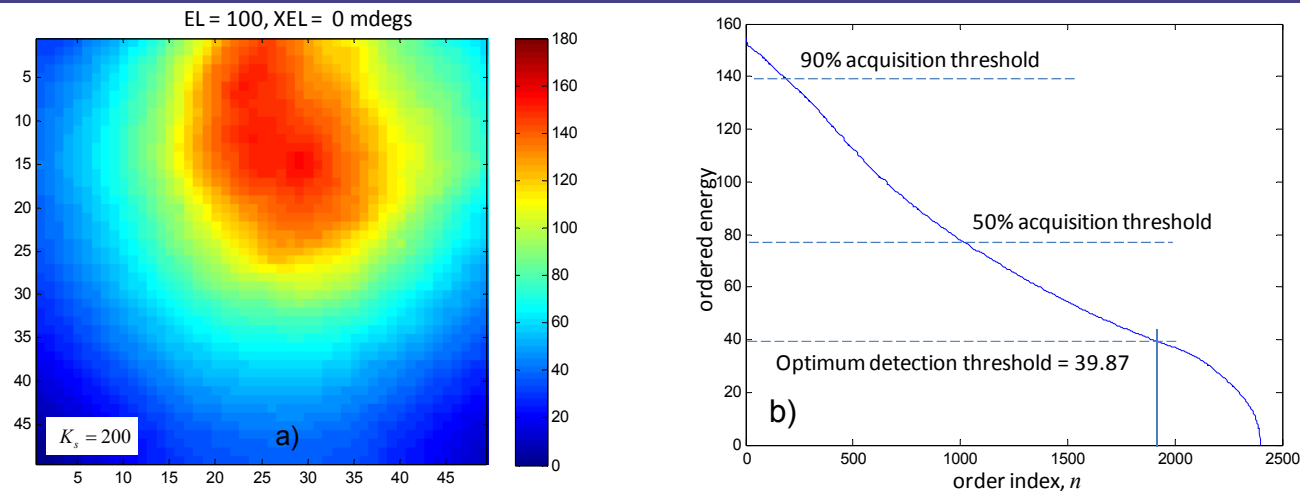
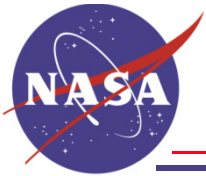
- without masking, using the entire array
- with various (1,0) masks defined as:
 - optimal detection mask
 - top 50% (order index)
 - top 90% (order index)

Cramer- Rao bound: Centroid estimation algorithms

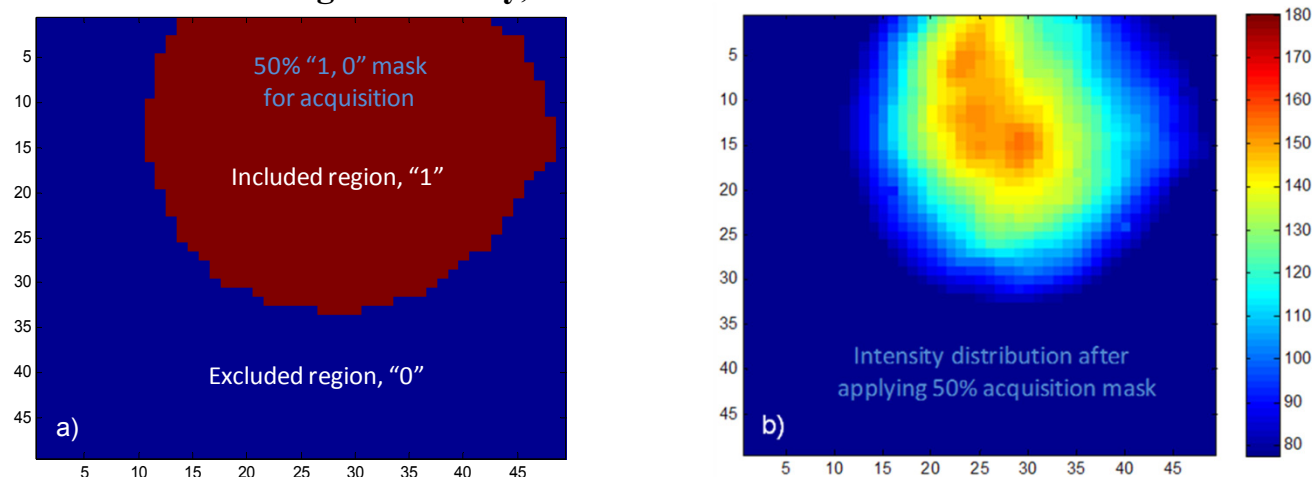
$$\text{var}(\hat{x}_0 - x_0) \geq \left\{ -E \left[- \sum_i \sum_j k_{ij} / \sigma_x^2 \right] \right\}^{-1} = \frac{\sigma_x^2}{\Lambda_s}$$

$$\text{var}(\hat{y}_0 - y_0) \geq \left\{ -E \left[- \sum_i \sum_j k_{ij} / \sigma_y^2 \right] \right\}^{-1} = \frac{\sigma_y^2}{\Lambda_s}$$

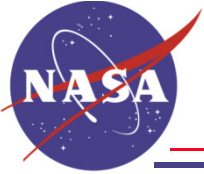
$$\sigma_x \equiv \sqrt{\text{var}(\hat{x}_0 - x_0)} \quad \sigma_y \equiv \sqrt{\text{var}(\hat{y}_0 - y_0)}$$



a) Initial PSF before centering, with 100 mdeg pointing error in elevation; b) Detector elements ordered according to intensity, as a function of the order index “ n ”.

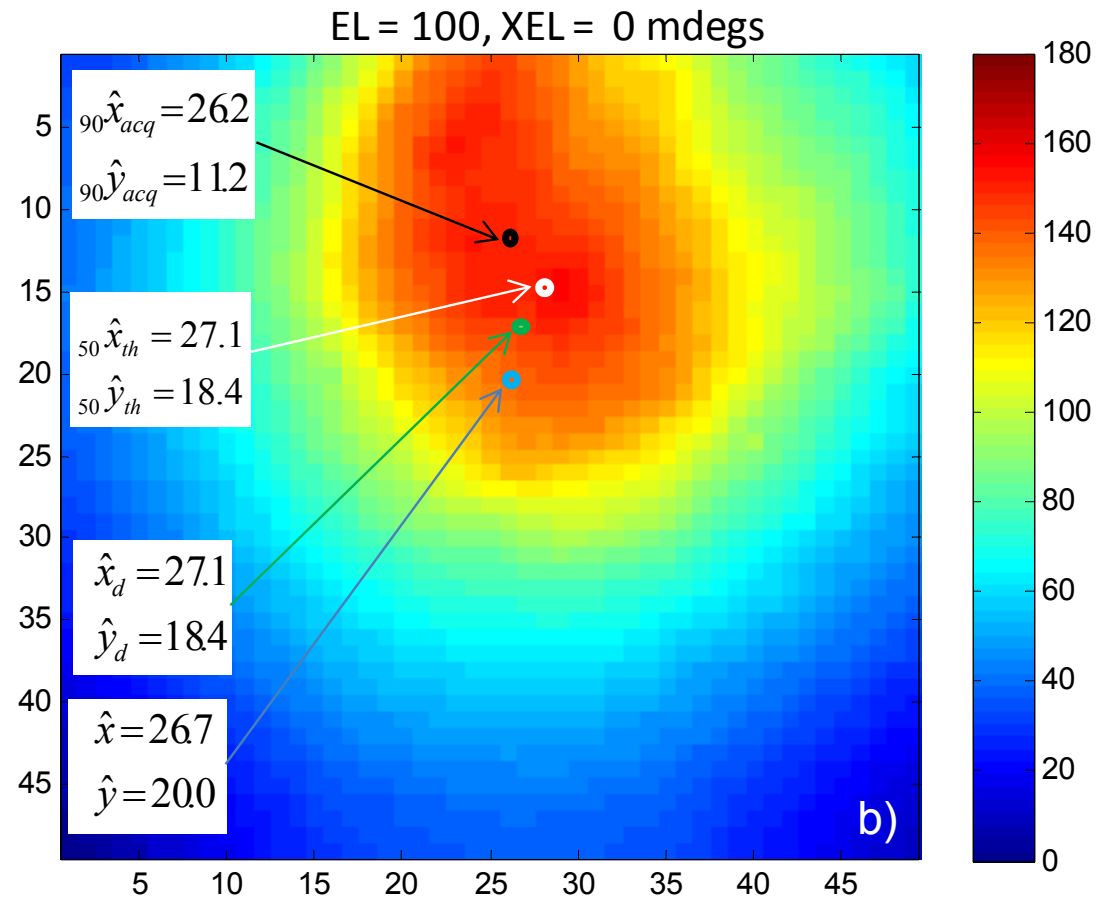


a) Simple “1, 0” mask obtained by including only those elements with order index less than 1900; modified intensity distribution after the detection mask is applied.

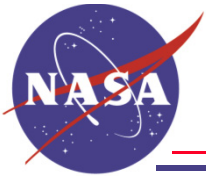


IEEE AEROSPACE CONFERENCE, MARCH 2012
Experimental Evaluation of "Polished Panel Optical Receiver" Concept

Jet Propulsion Laboratory
California Institute of Technology

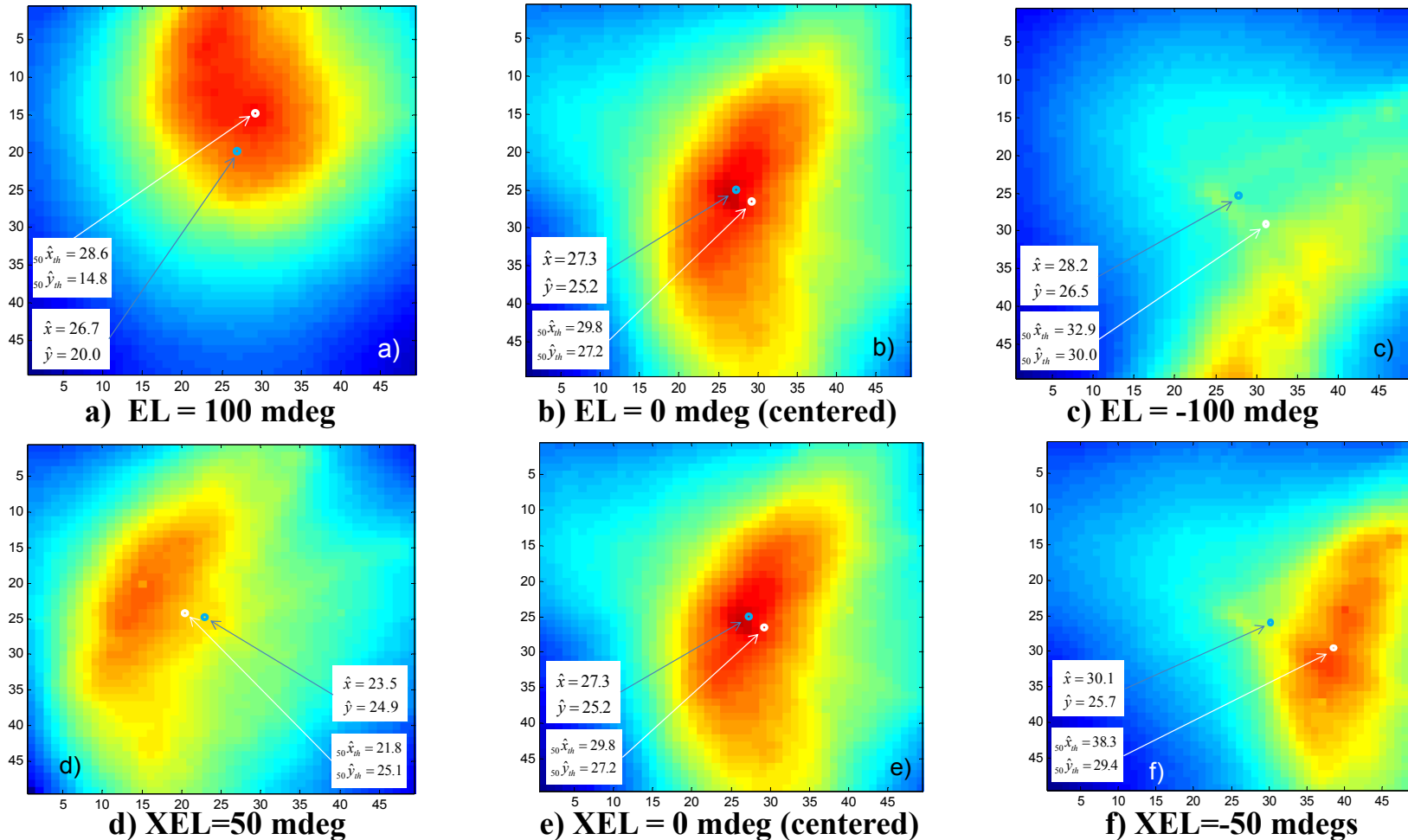


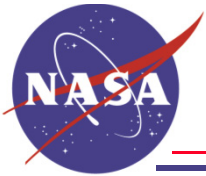
PSF center estimates obtained with the original centroid algorithm, detection-mask (1,0) algorithm, 50% and 90%-threshold (1,0) algorithms.



Response to Offsets and Centroid Algorithm Performance

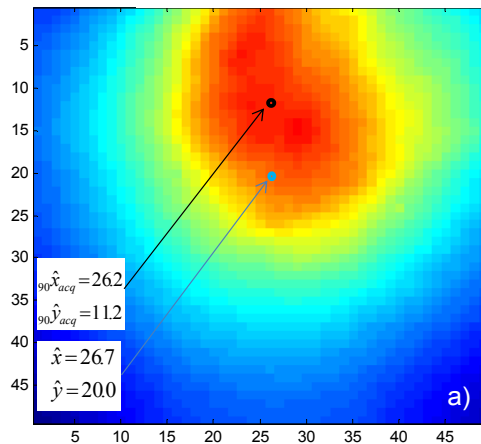
Original and 90%-threshold estimates, with elevation and cross-elevation offsets:



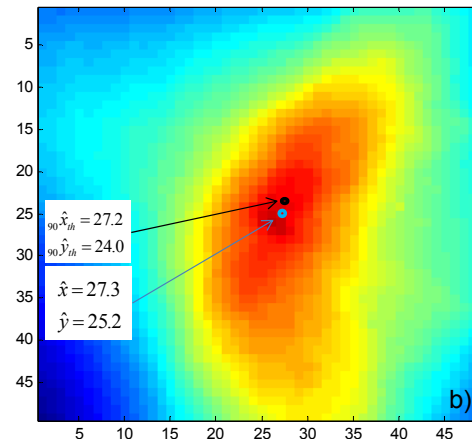


Response to Offsets and Centroid Algorithm Performance

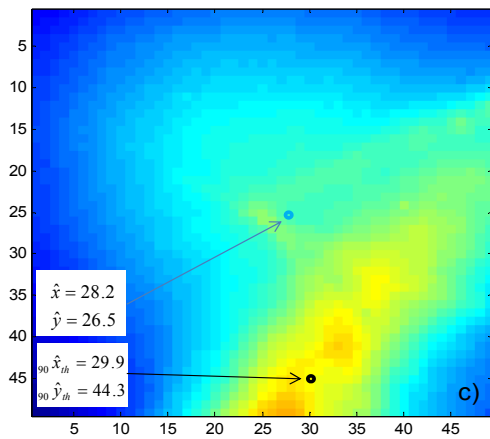
Original and 90%-threshold estimates, with elevation and cross-elevation offsets:



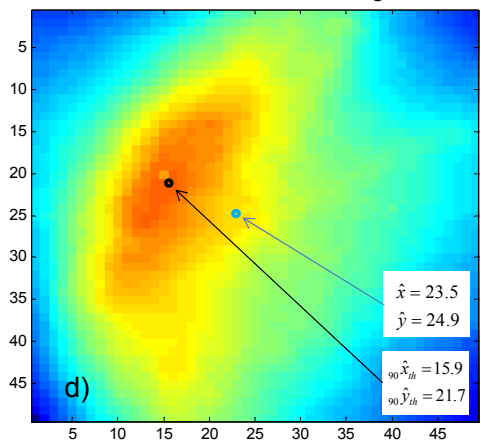
a) EL = 100 mdeg



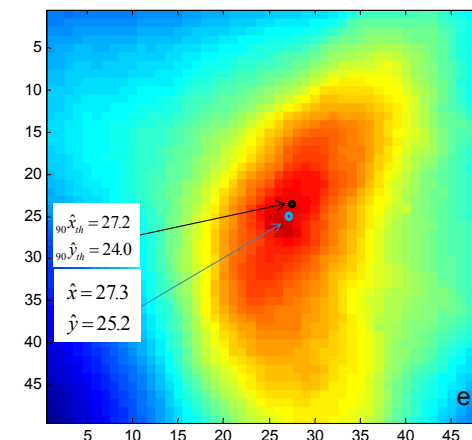
b) EL = 0 mdeg (centered)



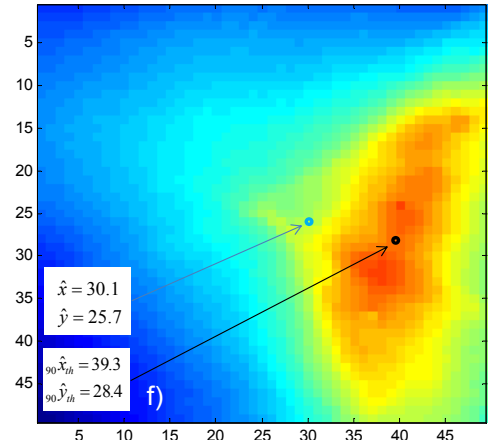
c) EL = -100 mdeg



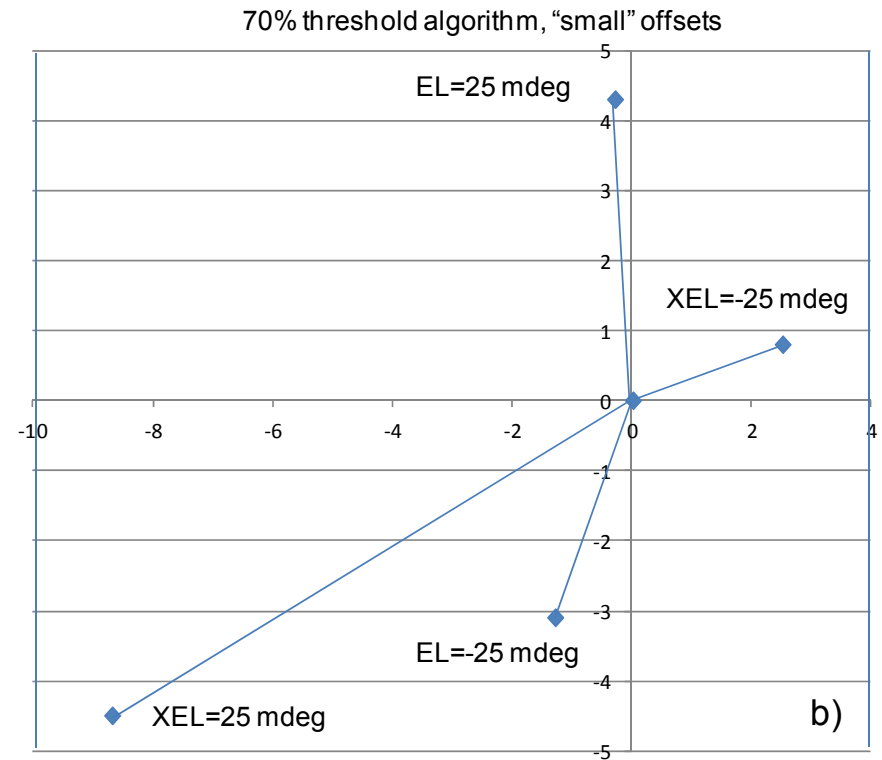
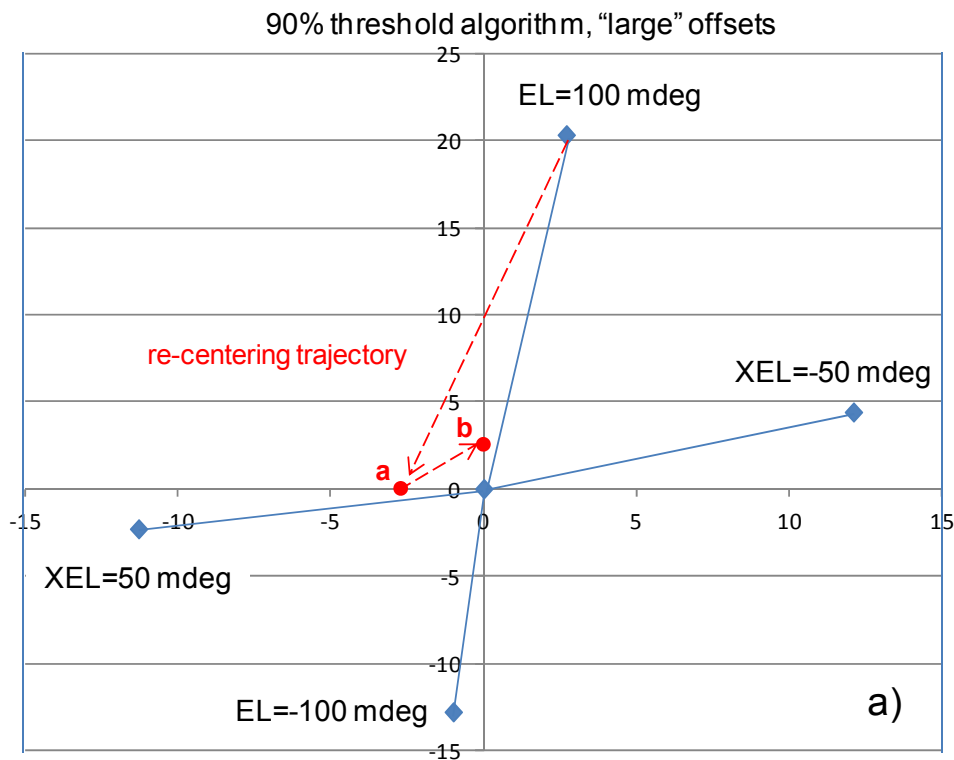
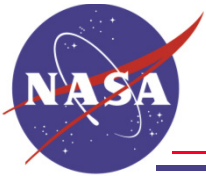
d) XEL = 50 mdeg



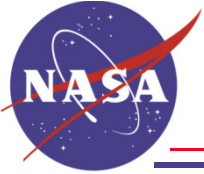
e) XEL = 0 mdeg (centered)



f) XEL = -50 mdeg



**Response of a) 90%-threshold algorithm to “large” offsets, and
b) 70%-threshold algorithm to “small” offsets, in the (XEL, EL) plane.**



	\hat{x}	\hat{y}	$_{70} \hat{x}_{th}$	$_{70} \hat{y}_{th}$	$_{90} \hat{x}_{th}$	$_{90} \hat{y}_{th}$
center	27.2	25.1	29.8	27.2	27.3	24.0
Δ – center	0	0	0	0	0	0
EL=25	-0.5	-1.1	-1.3	-3.1	-0.3	-1.9
EL=-25	0.0	0.6	-0.3	4.3	1.0	4.8
XEL=25	-3.0	-1.5	-8.7	-4.5	-4.4	-2.3
XEL=-25	0.0	-0.8	2.5	0.8	5.6	3.6

Summary of center estimates, and response to “small” offsets relative to center for the original, 70% and 90%-threshold centroid algorithms.